

TRAJECTORY GENERATION EXPERIMENTAL RESULTS OF A SINGLE TRACTION BALL MOBILE ROBOT

Edmundo Pozo Fortunic' / Gustavo Kato Ishizawa

Facultad de Ciencias e Ingeniería, Pontificia Universidad Católica del Perú

ABSTRACT

In this study, the preliminary experimental results of a single traction ball mobile robot are presented. The robot was designed, constructed and tested. A simple control system was developed to control the moving distance of the robot. The mobility experiments have been documented for further investigations.

Index Terms – Mobile robot, single traction ball, omnidirectional, experimental results

1. INTRODUCTION

Experimentations with a single traction ball for generation of omnidirectional locomotion are few. Lauwers, Kantor and Hollis [1], designed an inverse mouse-ball drive robot, designed a linear feedback controller and presented the results of the preliminary experimentations. Kumagai and Ochiai [2] developed a small robot that balanced on top of a ball. This robot is actuated by the use of three stepping motors that transmit the movement to the traction ball using omnidirectional wheels. Peng, Chiu, Tsai and Chou [3] designed also an omnidirectional spherical robot with a fussy controller for the balance control. Most of the studies related to the single traction ball are related to the balance control of the robot. On the other hand, few studies have been made in trajectory generation for this kind of mobile robots.

2. DESIGN OF THE SINGLE TRACTION BALL MOBILE ROBOT

The objective of the single traction ball robot is to move in any direction and be able to change it without making a twist. By the use of two perpendicular DC motors with rollers over a rubber ball, the robot is able to move in any direction by combining the spin of both actuators. Figure 2 shows the mechanical structure of the mobile robot. The structure is made of aluminum pieces of 10x8 cm (sides) that support the DC motors and rollers that keep the rubber ball fixed and a 10x10 cm (top) that carries the electronic circuit control board and battery packs.

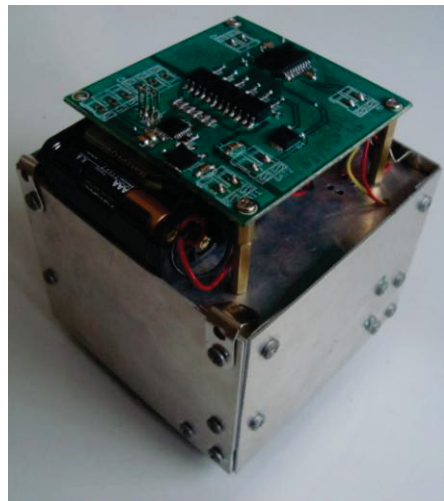


Figure 1: Single traction ball mobile robot.

The robot uses lightweight (10 g.) DC motors of 6V and 3000RPM (free run) and four metal ball casters as support wheels to keep the balance of the robot.

The circuit board is based on an ATMEGA88PA microcontroller and a L298 dual full-bridge driver that allows controlling both DC motors using time and PWM.

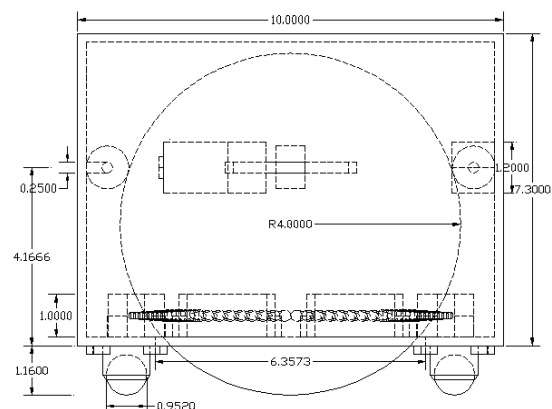


Figure 2: Structure of the mobile robot.

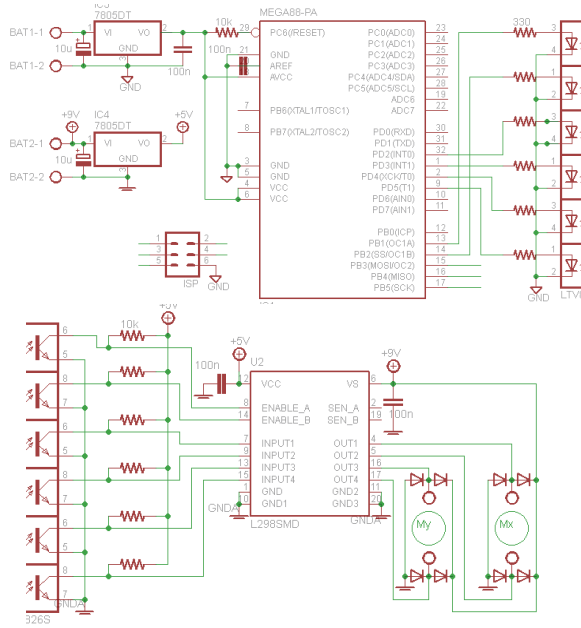


Figure 3: Circuit board Schematics

3. CONTROL SYSTEM

Using Newton's laws of linear and circular movement and DC motors equations, a theoretical model of the system was develop to analyze the possibilities of controlling the exact movement of the robot by the voltage applied to the motors. In this model, the rubber ball is rigid, the body structure is rigid, and there is no slip between the wheel and the floor and the wheel and the rollers. Also, it is assumed that there is no friction in the ball casters support wheels. Considering that the model has identical characteristics in both axis (X and Y) we can create a single model that will work for both and join them to create a full displacement system (plane XY).

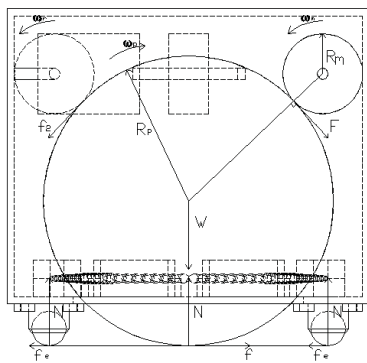


Figure 4: Free Body Diagram of the robot.

From tangential velocity relations:

$$\dot{x} = \omega_p r_p = \omega_m r_r \dots (1.1)$$

$$\ddot{x} = \dot{\omega}_p r_p = \dot{\omega}_m r_r \dots (1.2)$$

Where \dot{x} , \ddot{x} , ω_p , $\dot{\omega}_p$, ω_m , $\dot{\omega}_m$, r_p , r_r are respectively, the linear speed and acceleration of the system, the angular speed and acceleration of the ball, the angular

speed and acceleration of the motor, the ball radius and roller radius.

From Newton's second law of movement:

$$F = m_t \ddot{x} \dots (3)$$

Where F is the friction between the ball and floor and m_t is the total mass of the robot.

From the Free Body Diagram of the Ball:

$$T_m - T_f - 2T_r = I_p \dot{\omega}_p \dots (4)$$

Where T_m , T_f , T_r and I_p are respectively, the torque applied from the motor, the torque applied from the floor friction (which creates the motion), torque applied from the rollers and the moment of inertia from the ball.

From the motor's electric equations:

$$V = R_a i + V_b \dots (5.1)$$

$$V_b = K_b \omega_m \dots (5.2)$$

$$T_m = K_t i \dots (5.3)$$

Where V , R_a , i , V_b , K_b , K_t are respectively the voltage applied to the motor, the internal resistor, the motor current, the internal induced voltage, and the voltage induced-angular speed and torque-current constants.

Combining the equations (1) to (5) results in:

$$\frac{d\dot{x}}{dt} = - \frac{K_b K_t}{R_a r_r \left(\frac{2}{5} m_p r_p + m_r r_r + m_t r_p \right)} \dot{x} + \frac{K_t}{R_a \left(\frac{2}{5} m_p r_p + m_r r_r + m_t r_p \right)} V \dots (6)$$

Which allows the creation of a space-state model of the systems where state variables are the position and speed, and the voltage is the input.

$$\begin{bmatrix} \dot{x} \\ \dot{\dot{x}} \end{bmatrix} = \begin{bmatrix} 0 & 1 \\ - \frac{K_b K_t}{R_a r_r \left(\frac{2}{5} m_p r_p + m_r r_r + m_t r_p \right)} & 0 \end{bmatrix} \begin{bmatrix} x \\ \dot{x} \end{bmatrix} + \begin{bmatrix} 0 \\ \frac{K_t}{R_a \left(\frac{2}{5} m_p r_p + m_r r_r + m_t r_p \right)} \end{bmatrix} V$$

$$V = [1 \quad 0] X$$

Using the space-state model and transfer function associated to it, an equation establishing the relation between the voltage pulse time and distance traveled of the robot was created:

$$D = \frac{AT r_r}{K_b} \dots (7.1)$$

Where D , A , T are respectively, the distance traveled and the Amplitude and time of the voltage pulse.

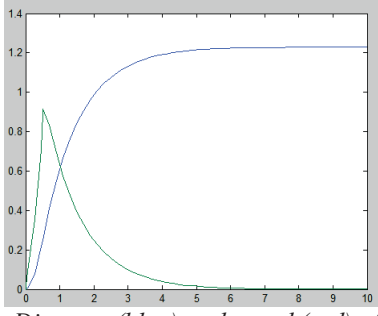


Figure 5: Distance (blue) and speed (red) of the robot from a 0.5s 6V pulse.

Considering that the distance travel settling time was long compared to the pulse time, an inverted voltage brake pulse was used to reduce that time; changing the system response and distance traveled.

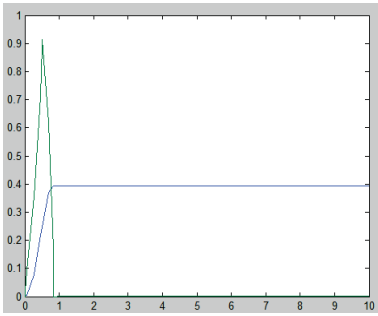


Figure 6: Distance (blue) and speed (red) of the robot from a 0.5s 6V pulse (+) and a 0.34s 6V brake pulse (-).

Changing the new distance relation to:

$$D = \frac{A(T - T_b)r_r}{K_b} \dots (7.2)$$

Where D , T and T_b are respectively, the distance traveled, the pulse time and the break pulse time. Considering that T_b has to be the exact time were the robot stops, the relation between T and T_b is determinate as:

$$T_b = \frac{\ln(2 - e^{-aT})}{a} \dots (8)$$

Where $a = \frac{K_b K_t}{R_a r_r (\frac{2}{5} m_p r_p + m_r r_r + m_t r_p)}$.

Recalculating D in terms of T and A gives:

$$D = \frac{A r_r}{a K_b} (aT - \ln(2 - e^{-aT})) \dots (9)$$

And T in terms of D and A gives:

$$T = \frac{-1}{a} \ln \left(1 - \sqrt{1 - e^{-\frac{a K_b (D)}{r_r}}} \right) \dots (10)$$

Which lets calculate the distance traveled of the robot through the pulse time and amplitude applied to the DC motor (without the need of feedback).

4. EXPERIMENTAL RESULTS

A number of tests were conducted to evaluate and characterize the performance of the mechanical and electronic control drive of the robot, which were divided into 3 groups according to its nature and difficulty. The Straight line movement experiments were designed to evaluate the performance of the displacement of the robot in a single direction controlled by a single motor at a time (tested in both ways for both motors). The Sideway movement experiments were designed to evaluate the performance of the displacement of the robot in a single direction controlled by both motors (the four combinations were tested). The Circular movement experiments were designed to evaluate the performance of the displacement of the robot in a sequence of multiple directions, which is the highest requirement for the robot.

4.1. Straight line movement experiments

The experiments are separated into 4 cases: EAST (E) and WEST (W) movements that require the X motor; and NORTH (N) and SOUTH (S) movements that require the Y motor. Each case has 3 distances experiments repeated 10 times. Table 1 shows the means of the experimental results obtained; where the E case moves considerably more than expected.

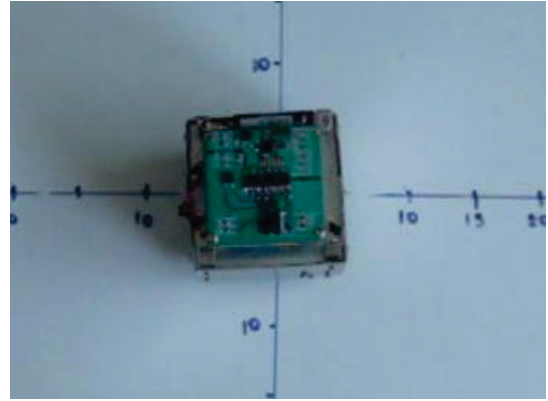


Figure 7: Straight line movement: Initial Position

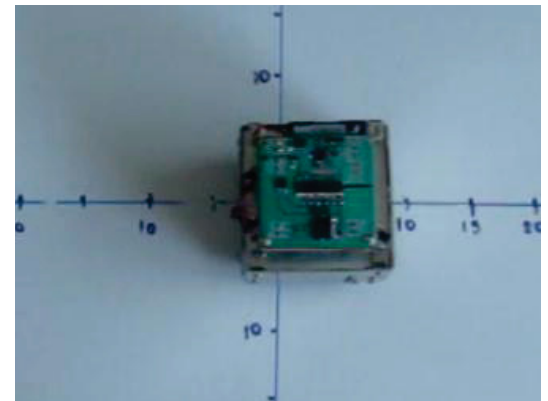


Figure 8: Straight line movement: Transitive Position

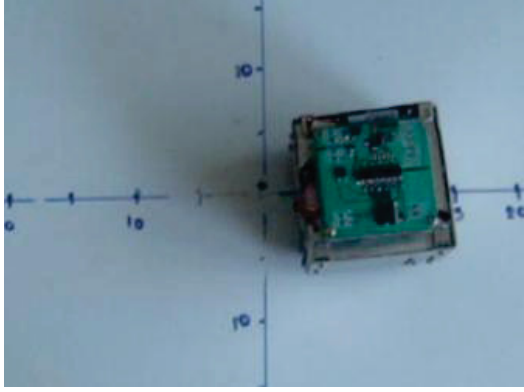


Figure 9: Straight line movement: Final Position

Movement	Distance (cm)		
	4	12	20
E	9.6	23.7	40
W	2.7	5.6	16
N	3.3	10.8	19.4
S	3.3	10.3	19.4

Table 1: Experimental straight line mean distances.

4.2. Sideway movement experiments

The experiments are separated in 4 cases: NE, NW, SW and SE which are the combination of the previous straight line movements that uses the different rotations of both X and Y motors.

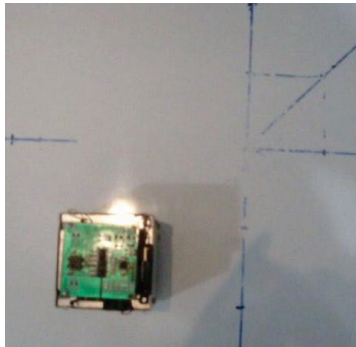


Figure 10: Sideway movement: Initial position



Figure 11: Sideway movement: Transitive position

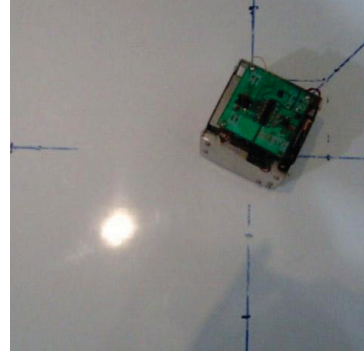


Figure 12: Sideway movement: Final position

Movement	Distance(cm)		
	5.7	17.0	28.3
NE	15.3	23.4	29.5
NW	5.6	12.1	16.6
SW	0*	0*	0*
SE	6.9	20.5	34.1

Table 2: Experimental sideways mean distances.

As seen in the straight line results, the NE shows the “excess of movement” component from the E movement.

*Due to the continued experimentation, the rubber ball got a bit deflated and when the rollers moved the ball in the SW combination, the ball got stuck up, leaving no contact with the ground.

4.3. Circular movement experiments

Using the approximation to curves as the sum of short line segments, a circular trajectory was planned using a combination of the previous movement as a way to evaluate the response efficiency of the robot’s mechanical structure in a multiple directions task.

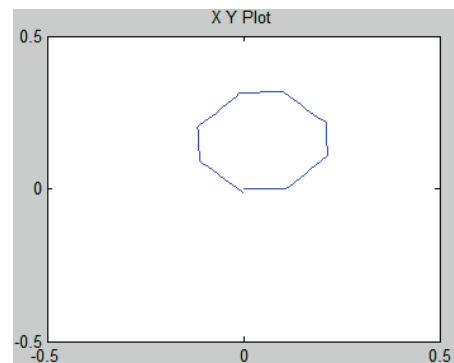


Figure 13: Circular movement simulation.

As shown in Figure 12, the robot was programmed to do the straight line and sideways movements in a combined order (E, NE, N, NW, W, SW, S, SE) to create the hexagonal-circular movement.

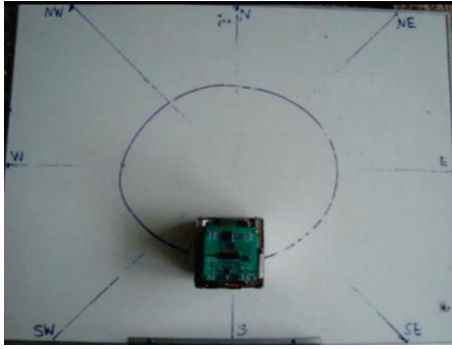


Figure 14: Circular movement: start position.

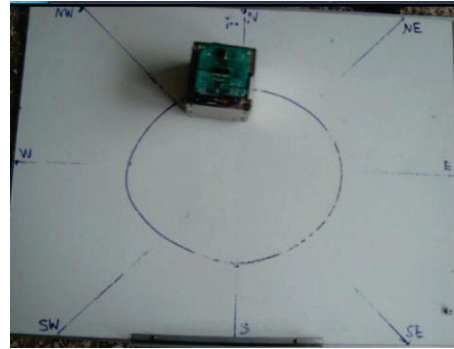


Figure 18: Circular movement: Transitive position 4

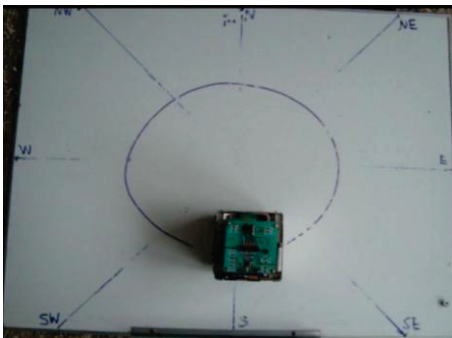


Figure 15: Circular movement: Transitive position 1

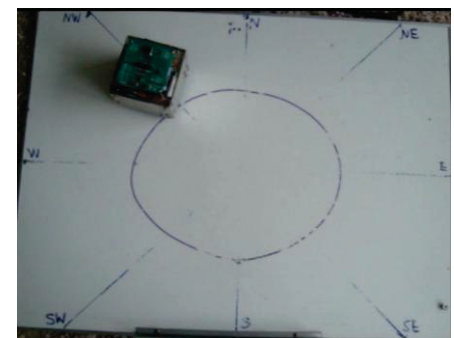


Figure 19: Circular movement: Transitive position 5

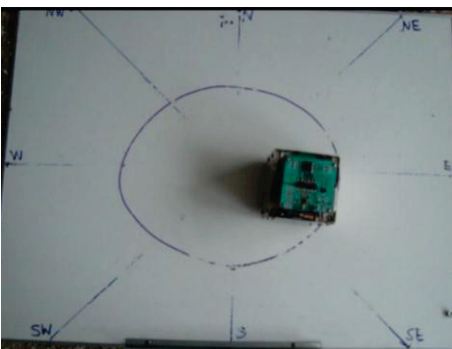


Figure 16: Circular movement: Transitive position 2

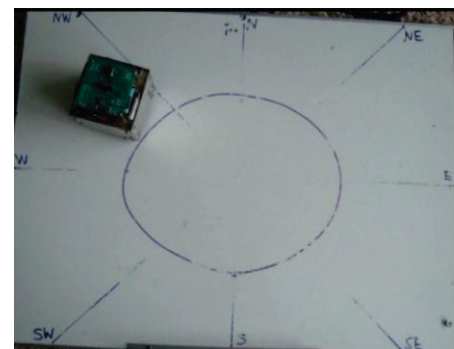


Figure 20: Circular movement: Transitive position 6

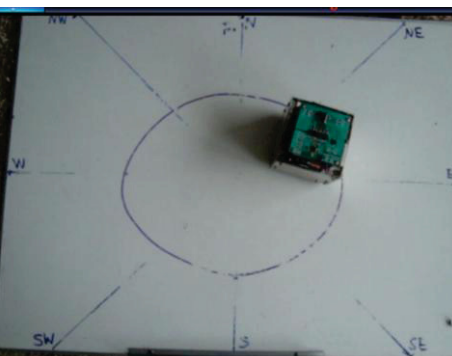


Figure 17: Circular movement: Transitive position 3

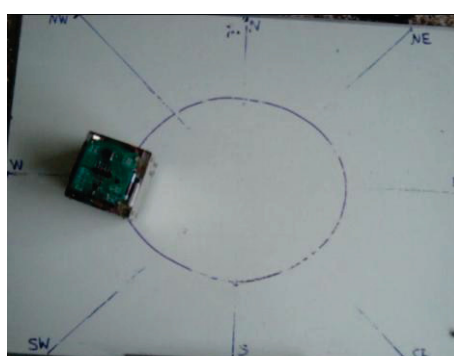


Figure 21: Circular movement: final position

Although it was programmed to return to its original position, the robot wasn't able and finished in a near-like position following a similar circular-hexagonal movement as expected.

5. CONCLUSIONS

The single traction ball robot was able to move in a series of different direction and distance movements according to its programming; however, it is also shown a low precision in distances, no symmetry in displacement and a no displacement case (SW) due to mechanical errors and assembly problems.

6. FUTURE WORK

Since the electronic control board design is sufficient to control the motors used in the mechanical drive of the single traction ball, but the mechanical drive developed is not sufficient to realize an accurate study of the omnidirectional displacement system due to assembly and design problems; it is possible to develop a new one to continue the studies.

7. REFERENCES

- [1] Lauwers, Cantor and Hollis, "A Dynamically Stable Single-Wheeled Mobile Robot with Inverse Mouse-Ball Drive", Proceedings of IEEE International Conference on Robotics and Automation, ISSN: 1050-4729, USA, pp. 2884-2889, 2006.
- [2] Kumagai and Ochiai, "Development of a Robot Balanced on a Ball – First Report", Journal of Robotics and Mechatronics, ISSN: 0915-3942, Japan, Vol.22, No.3, 2010.
- [3] Peng, Chiu, Tsai and Chou, "Design of an Omnidirectional Spherical Robot Using Fuzzy Control", Proceedings of the International Multiconference of Engineers and Computer Scientists (IMECS), ISBN: 978-988-17012-2-0, Hong Kong Vol.1, 2009.